ChemComm

ROYAL SOCIETY OF CHEMISTRY

COMMUNICATION

View Article Online
View Journal | View Issue

Check for updates

Cite this: *Chem. Commun.*, 2024, **60**, 866

Received 5th December 2023,
Accepted 15th December 2023

DOI: 10.1039/d3cc05934k

rsc.li/chemcomm

Published on 18 december 2023. Downloaded on 12.2.2026. 20.02.24.

Tailoring fluorescent ZIF-8 nanostructures through calix[4]pyrrole modification: tunable size and enhanced organic micropollutant removal capacity†

Nida Ük,[a] Fatma Yelda Ünlü,[b] Özge İbiş,[b] Ilgın Nar,[c] Abdullah Aydogan*[b] and Caner Ünlü*[ab]

Whitish-blue light emitting fluorescent ZIF-8 structures were synthesized by means of bis-carboxylate functional calix[4]pyrrole (BCCP) modification. The calix[4]pyrrole concentration was also manipulated to tune the sizes of the ZIF-8 structures. Moreover, the BCCP-modified ZIF-8 samples exhibited enhanced organic micropollutant removal capacity from aqueous solutions.

Due to their tunable porous structures and high surface areas, zeolitic imidazolate framework-8 (ZIF-8) structures are well-known versatile metal–organic frameworks that are considered excellent candidates for various applications including organic micropollutant removal and gas adsorption studies.[1–4] Despite possessing unique properties, the absence of inherent fluorescence makes ZIF-8 structures impractical for technologies that rely on light emission, such as optical sensing, imaging, and optoelectronic devices.[5–7] In recent years, numerous studies have been conducted to impart fluorescence properties *via* modification of ZIF-8 structures with fluorescent molecules or photonic nanocrystals, organic dyes, and quantum dots.[5–11]

Calix[4]pyrroles are versatile macrocyclic compounds consisting of four pyrrole units connected to each other *via* substituted methylene bridges.[12] The specific ability of calix[4]pyrroles to bind anions through hydrogen bonding consolidated their place in various applications including molecular recognition,[13] sensing,[14] and supramolecular chemistry.[15] Among their numerous derivatives, carboxylic acid-functionalized calix[4]pyrroles have primarily been preferred as starting materials for further derivatization of these macrocycles.[16,17] Calix[4]pyrroles were also demonstrated in designing crystalline, porous organic materials.[18] However, they are yet to be considered as modifiers for well-known MOF structures, such as ZIF-8. This is mainly because their macro-size and rigid structure could putatively deform the MOF structure, which may lead to formation of defects in the crystal and the porous structure of the desired MOFs.[19,20]

In this study, non-modified and modified ZIF-8 structures were synthesized by adapting a traditional method frequently used in the literature.[1–4] For the modification, a fluorescent calix[4]pyrrole compound tethered with two carboxylate units (BCCP), in the form of its tetrabutylammonium (TBA) salt,[21] was used (Scheme 1). Briefly, BCCP was added directly to a DMF solution containing 2-methylimidazole (mIM) during the synthesis of ZIF-8 samples at room temperature with a BCCP:mIM ratio of 1 : 80 at the most. To understand the effect of BCCP on the structure of ZIF-8, 0.1 and 0.01 mmol BCCP were used and

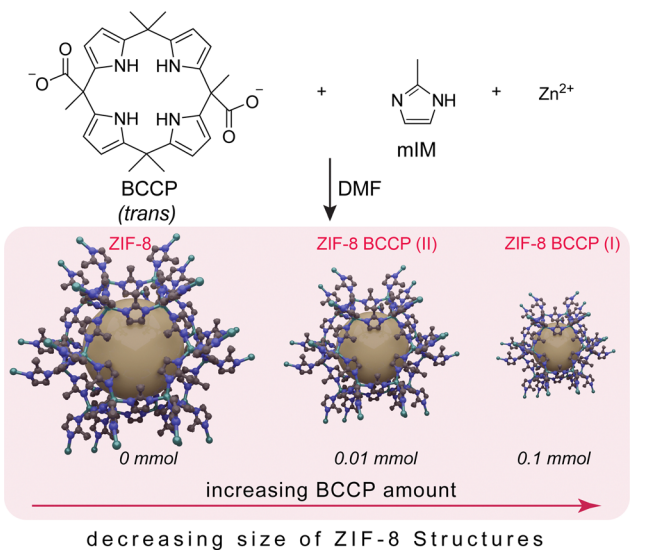

Scheme 1 Schematic illustration showing the synthesis of BCCP-modified ZIF-8 structures.

[a] *Department of Polymer Science and Technology, Istanbul Technical University, Maslak, 34469, Istanbul, Turkey. E-mail: canerunlu@itu.edu.tr, aydoganab@itu.edu.tr*
[b] *Department of Chemistry, Istanbul Technical University, Maslak, 34469, Istanbul, Turkey*
[c] *Istanbul Technical University Nanotechnology Research and Application Center (ITUNano), Istanbul, Turkey*

† Electronic supplementary information (ESI) available. See DOI: https://doi.org/10.1039/d3cc05934k

This journal is © The Royal Society of Chemistry 2024

Published on 18 december 2023. Downloaded on 12.2.2026. 20.02.24.

the resulting ZIF-8 samples were labelled as ZIF-8 BCCP(I) and ZIF-8 BCCP(II), respectively. After that, several characterizations were performed for both BCCP-modified and non-modified ZIF-8 samples (see ESI† for details of preparations, and for ^{1}H- and ^{13}C-NMR spectra of BCCP).

The XRD pattern of the non-modified ZIF-8 matches that of cubic ZIF-8 (JCPDS 00-062-1030)[22] (Fig. 1, the XRD peaks and their attributed planes are defined in the ESI†). As BCCP integrated into the ZIF-8 structure, there were significant changes in peak widths and intensity ratios in the XRD spectrum (Fig. 1). When non-modified ZIF-8 is considered, the most intense peak was observed at 7.34°, corresponding to the (110) plane. The traditional ZIF-8 structures exhibit a dominant geometry of the (110) plane, which is a consequence of their thermodynamically stable crystal structure and the repetition of the unit cells along the (110) axis (Fig. 1).[23,24] However, the most intense peaks in the XRD spectra of the BCCP-modified ZIF-8 samples were observed at 12.75°, corresponding to the (211) plane (Fig. 1). These results allowed us to suggest that the BCCP integrated into the ZIF-8 structure and hindered the repetition of the unit cells on the (110) plane. As a result, the ZIF-8 crystals were unable to grow on the (110) plane, leading to a reduction in the size and the presence of Zn–mIM linkages on the crystal surface, which are naturally present in the (211) plane.[24] In addition, it should be noted that BCCP exhibits a unique crystal-like structure on its own above a certain concentration (0.1 M), as reported in the literature.[21] On the other hand, the maximum concentration of BCCP used in this study was 0.01 M, hindering formation of crystalline BCCP. Furthermore, the XRD spectrum of ZIF-8 exhibited broadening in all peaks after its modification with BCCP. The full width at half maximum (FWHM) of the peak at 7.34° increased from 0.10 degrees to 0.21 degrees in the case of ZIF-8 BCCP(II) and to 0.42 degrees in the case of ZIF-8 BCCP(I). In the context of nanocrystals, broadening of the XRD peaks often signifies a reduction in their size. Therefore, these findings suggest that the crystal size becomes smaller when ZIF-8 is subjected to BCCP modification, and it is evident that the amount of BCCP has a significant impact on the size of modified ZIF-8 structures.

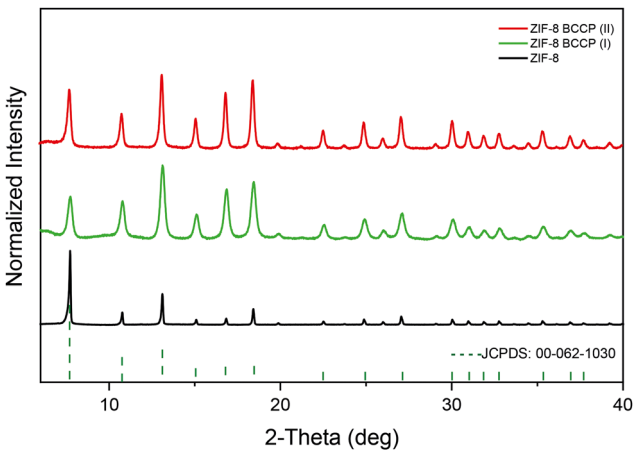

Fig. 1 XRD spectra of non-modified ZIF-8 and BCCP-modified ZIF-8.

A scanning electron microscopy (SEM) image of the non-modified ZIF-8 nanocrystals is given in Fig. 2a and exhibits an average size of around 270 nm and maintains a cubic structure. When the ZIF-8 structures were subjected to BCCP modification, their morphology remained unchanged (Fig. 2b–d); however, a substantial reduction in their sizes became apparent. While the average size of ZIF-8 BCCP(II) was found to be 140 nm, it decreased to 65 nm in the case of ZIF-8 BCCP(I), where the molar ratio of BCCP was the highest (for TEM image of ZIF-8 BCCP(I), see Fig. S1, ESI†). These findings are in accordance with the data obtained from XRD and emphasize the ability to control the size of ZIF-8 by regulating the concentration of BCCP. Furthermore, the BET analysis pointed out that the surface characteristics of ZIF-8 entirely changed as BCCP was integrated into ZIF-8. While the surface area of modified ZIF-8 slightly decreased after BCCP modification, the pore size and pore volume significantly decreased in BCCP-modified ZIF-8, pointing out that the decrease in crystalline size caused a decrease in the pore size corresponding to a significant increase in cumulative surface area of pores and entirely different adsorption/desorption characteristics (see ESI† and Fig. S2 for BET results). The non-modified ZIF-8 exhibited typical type I isotherms, which was characteristic of adsorption in microporous materials and frequently observed in ZIF-8 materials.[1–4] However, BCCP-modified ZIF-8 structures pronounce a type IV adsorption isotherm, which is characteristic of mesoporous materials, as a consequence of reduction in pore size.

FTIR spectra of BCCP-modified ZIF-8, and non-modified ZIF-8 are shown in Fig. S3 (ESI†) and reveal that the TBA counter-cations of BCCP are not present in the BCCP-modified ZIF-8 structures when the above spectra are compared with that of BCCP (Fig. S3, ESI†). A significant decrease in the intensity of aliphatic C–H bands around 2900 cm^{-1} and the broad band around 3400 cm^{-1} (Fig. S3, ESI†) supports the above conclusion. The Raman spectra of non-modified- and modified-ZIF-8 structures are depicted in Fig. S3 (ESI†). While the spectrum of

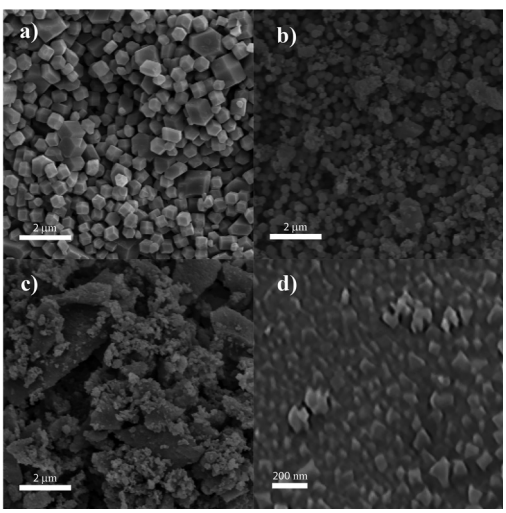

Fig. 2 SEM images of (a) non-modified ZIF-8, (b) ZIF-8 BCCP(II), (c) ZIF-8 BCCP(I) and (d) ZIF-8 BCCP(I) with higher resolution.

Published on 18 december 2023. Downloaded on 12.2.2026. 20.02.24.

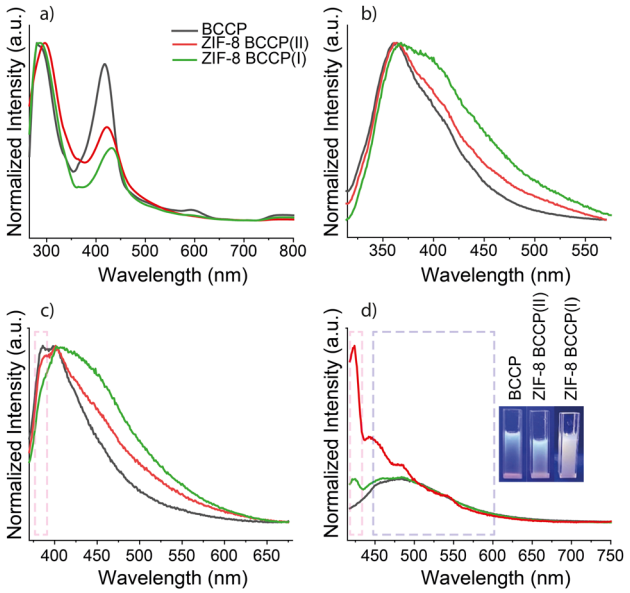

Fig. 3 (a) Absorption spectra of non-modified ZIF-8 and BCCP-modified ZIF-8. Fluorescence spectra of BCCP and BCCP-modified ZIF-8 samples at different excitation wavelengths: (b) 300, (c) 350, and (d) 400 nm. Inset: illumination of BCCP and BCCP-modified ZIF-8 under UV-light (366 nm). All emission spectra were normalized to 1 at the most intense peak point.

non-modified ZIF-8 matched exactly with the data reported in the literature,[25] the spectra of BCCP-modified ZIF-8 were almost identical with the spectrum of non-modified ZIF-8. However, the emergence of a new peak around 1560 cm^{-1} was attributed to the pyrrole rings of BCCP (Fig. S3, ESI†) and considered as further proof of the BCCP-ZIF-8 hybrid structure.[26]

The absorption spectra of BCCP and BCCP-modified ZIF-8 structures are given in Fig. 3 and exhibit significant differences. The absorption spectrum of BCCP showed two maxima with almost equal intensity at 295 and 417 nm (Fig. 3a). Typically, absorption peaks in the 295 nm range could be associated with π–π* transitions in C═C double bonds belonging to pyrrole rings and the peak at 417 nm could be attributed to the organized crystal-like structure of BCCP.[21] The ratio of the absorbance at 417 nm to the absorbance at 295 nm was found to be reduced after the modification of ZIF-8 with BCCP. This was considered as further evidence of BCCP participation in the modified ZIF-8 structures and the disappearance of the organized BCCP assembly. The evidence of the participation was also confirmed from the absorption peaks at longer wavelengths exhibiting a slight red-shift with an increase in the concentration of BCCP.

The non-modified ZIF-8 structures do not display any fluorescence properties and are insoluble in DMF, which are characteristics of ZIF-8.[1,2] In contrast, BCCP-modified ZIF-8 structures were slightly soluble in DMF and had fairly bright whitish blue emission upon excitation with a 366 nm laser (inset of Fig. 3d). The origin of the fluorescence emission in modified ZIF-8 was the BCCP molecule and it had an excitation-dependent emission feature (Fig. 3b–d). It possessed dual emission properties with an intense peak at 366 nm and a shoulder peak at around 400 nm upon excitation with 300 nm. It also had a broad single fluorescence peak at 400 nm with an FWHM of 75 nm upon excitation with 350 nm. Upon excitation with 400 nm, a broad single fluorescence peak at 485 nm with an FWHM of 105 nm was also observable. The quantum yield (QY) of BCCP was calculated to be 1.2%. The non-modified ZIF-8 became fluorescent with different photophysical properties as BCCP integrated into the ZIF-8 structure (*cf.* Fig. 3b and c). The emission spectrum of BCCP-modified ZIF-8 enounced an increased quantum yield (around 7.3%) and significant differences at 300, 350 and 400 nm excitations compared to those of BCCP. When the BCCP-modified ZIF-8 was excited at 300 nm, the emission peak of BCCP-modified ZIF-8 becomes broader and the intensity of the shoulder peak at 400 nm increases. Almost similar behaviour was also observed when BCCP-modified ZIF-8 was excited at 350 nm. In the case of excitation at 400 nm, BCCP-modified ZIF-8 pronounced more noticeable differences, such as emergence of a new peak at 420 nm and a decrease in the relative intensity of the peak at 485 nm depending on the decreasing concentration of BCCP in ZIF-8. Consequently, the emission colour became closer to white light due to the broadening of the existing and the appearance of new emission peaks (Fig. 3). In addition, the characteristics of the photoluminescence excitation (PLE) spectrum show significant differences upon integration of BCCP into the ZIF-8 structure which are discussed in the ESI† (Fig. S4).

BCCP possesses two carboxylate groups and is soluble in water (Fig. S5, ESI†). In contrast, BCCP-modified ZIF-8 structures were found to be insoluble in water, while they were slightly soluble in DMF (Fig. S5, ESI†). Given the solubility of BCCP-modified ZIF-8 in DMF, these materials hold promise for investigations focusing on the emission properties of ZIF-8. Conversely, the insolubility of BCCP-modified ZIF-8 in water could make it potentially valuable for organic micropollutant removal studies because previous research demonstrated that ZIF-8 could remove a cationic organic micropollutant, rhodamine B, with a high removal efficiency from the aqueous environment because of the affinity of imidazole groups to rhodamine B.[27,28] In our study, the organic micropollutant removal properties of both modified and non-modified ZIF-8 were evaluated with three distinct cationic organic micropollutants (Fig. 4): rhodamine B (RB), methylene blue (MB), and methyl violet 2B (MV).

As anticipated, non-modified ZIF-8 removed a certain percentage of RB (70%). However, after BCCP modification, the removal efficiency of ZIF-8 for RB noticeably decreased. While the removal efficiency of ZIF-8 BCCP(I) was 25%, it was found to be 11% in the case of ZIF-8 BCCP(II). These results indicate that the presence of BCCP in the ZIF-8 structure significantly altered the interaction between ZIF-8 and RB. Conversely, a completely different scenario was observed with MB and MV. While the non-modified ZIF-8 did not remove any MV and removed 33% of MB, modified ZIF-8 exhibited a substantially higher removal efficiency for both organic micropollutants. As the BCCP content in ZIF-8 increased, so did the removal capacity. For BCCP ZIF-8(II), the removal efficiencies were 80% for MB and 37% for MV. In the case of BCCP ZIF-8(I), where the BCCP concentration was higher, the removal efficiencies were 96% for MB and 60% for MV (see ESI† for calculation of removal efficiencies).

 This journal is © The Royal Society of Chemistry 2024

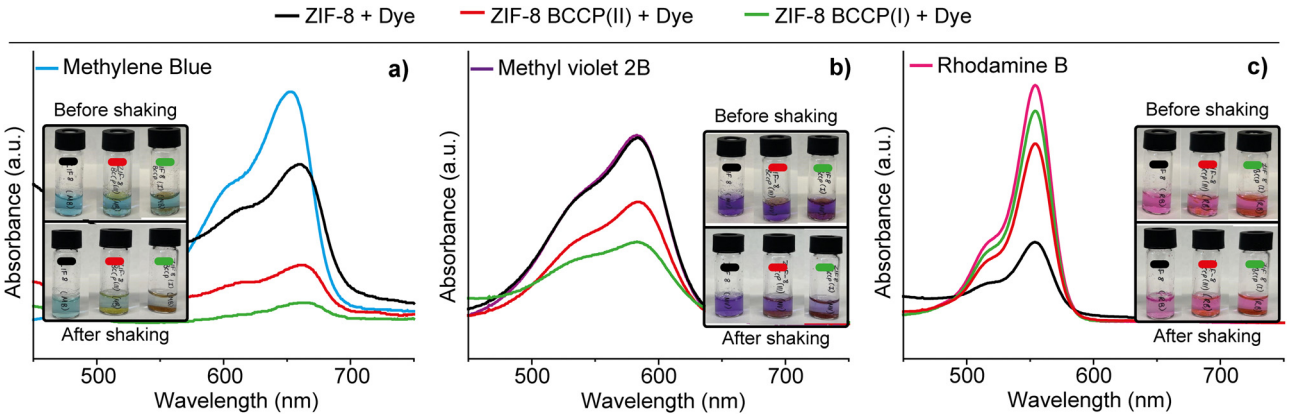

Fig. 4 Absorption spectra of organic micropollutants: (a) methylene blue, (b) methyl violet 2B, and (c) rhodamine B before and after treatment with ZIF-8 structures. The insets show the aqueous solutions of dyes before (top layers) and after shaking (bottom layers) with ZIF-8 structures for 2 hours: (left) methylene blue, (middle) methyl violet 2B, and (right) rhodamine B.

Published on 18 december 2023. Downloaded on 12.2.2026. 20.02.24.

These results highlighted that BCCP modification entirely transformed the characteristics of ZIF-8 with respect to the high affinity of calix[4]pyrrole to MB and MV,[29] allowing the adjustment and customization of ZIF-8's organic micropollutant removal properties to suit various pollution scenarios in different environments.

In conclusion, fluorescent BCCP-modified ZIF-8 structures were successfully synthesized by modifying the traditional ZIF-8 synthesis process. These novel ZIF-8 structures emit a vibrant whitish-blue colour when exposed to UV light. Their sizes ranged from 65 to 270 nm and could be controlled by adjusting the BCCP concentration in the synthesis medium. The ZIF-8 and modified ZIF-8 had the capacity to remove organic micropollutants from aqueous environments, which could be manipulated by BCCP modification.

This work is funded by TUBİTAK – BIDEB under the 2244 programme with grant number: 119C197.

Conflicts of interest

There are no conflicts to declare.

Notes and references

1 K. S. Park, Z. Ni, A. P. Côté, J. Y. Choi, R. Huang, F. J. Uribe-Romo, H. K. Chae, M. O'Keeffe and O. M. Yaghi, *Proc. Natl. Acad. Sci. U. S. A.*, 2006, **103**, 10186–10191.
2 G. Lu, S. Li, Z. Guo, O. K. Farha, B. G. Hauser, X. Qi, Y. Wang, X. Wang, S. Han, X. Liu, J. S. Duchene, H. Zhang, Q. Zhang, X. Chen, J. Ma, S. C. J. Loo, W. D. Wei, Y. Yang, J. T. Hupp and F. Huo, *Nat. Chem.*, 2012, **4**, 310–316.
3 F. Lyu, Y. Zhang, R. N. Zare, J. Ge and Z. Liu, *Nano Lett.*, 2014, **14**, 5761–5765.
4 H. L. Jiang, B. Liu, T. Akita, M. Haruta, H. Sakurai and Q. Xu, *J. Am. Chem. Soc.*, 2009, **131**, 11302–11303.
5 Q. Liu, S. Tian, X. Zhao and G. Sankar, *J. Mater. Chem. C*, 2021, **9**, 5819–5826.
6 Y. Xia, Y. Hong, R. Geng, X. Li, A. Qu, Z. Zhou and Z. Zhang, *ACS Omega*, 2020, **5**, 3478–3486.
7 Y. Si, Y. Li, G. Yang, S. Zhang, L. Yang, W. Dai and H. Wang, *Anal. Chim. Acta*, 2022, **1199**, 339576.
8 X. Lin, G. Gao, L. Zheng, Y. Chi and G. Chen, *Anal. Chem.*, 2014, **86**, 1223–1228.
9 Z. Tian, X. Yao, K. Ma, X. Niu, J. Grothe, Q. Xu, L. Liu, S. Kaskel and Y. Zhu, *ACS Omega*, 2017, **2**, 1249–1258.
10 B. P. Biswal, D. B. Shinde, V. K. Pillai and R. Banerjee, *Nanoscale*, 2013, **5**, 10556–10561.
11 Y. Shu, Q. Ye, T. Dai, Q. Xu and X. Hu, *ACS Sens.*, 2021, **6**, 641–658.
12 P. A. Gale, J. L. Sessler, V. Král and V. Lynch, *J. Am. Chem. Soc.*, 1996, **118**, 5140–5141.
13 D. S. Kim and J. L. Sessler, *Chem. Soc. Rev.*, 2015, **44**, 532–546.
14 S. Amharar and A. Aydogan, *Dyes Pigm.*, 2022, **197**, 109918.
15 I. A. Rather, S. A. Wagay, M. S. Hasnain and R. Ali, *RSC Adv.*, 2019, **9**, 38309–38344.
16 J. Lee, J. T. Brewster, B. Song, V. M. Lynch, I. Hwang, X. Li and J. L. Sessler, *Chem. Commun.*, 2018, **54**, 9422–9425.
17 J. Aguilera-Sigalat, C. Sáenz De Pipaón, D. Hernández-Alonso, E. C. Escudero-Adán, J. R. Galan-Mascarós and P. Ballester, *Cryst. Growth Des.*, 2017, **17**, 1328–1338.
18 L. P. Skala, C. L. Stern, L. Bancroft, C. M. Moisanu, C. Pelkowski, X. Aguilar-Enriquez, J. L. Swartz, M. R. Wasielewski and W. R. Dichtel, *Chem*, 2023, **9**, 1208–1220.
19 P. A. Gale, J. L. Sessler and V. Král, *Chem. Commun.*, 1998, 1–8.
20 P. A. Gale, P. Anzenbacher and J. L. Sessler, *Coord. Chem. Rev.*, 2001, **222**, 57–102.
21 F. Yelda Ünlü and A. Aydogan, *Macromol. Rapid Commun.*, 2022, **43**, 2200447.
22 S. Sharma and P. Chand, *Mater. Today: Proc.*, 2023, **76**, 125–131.
23 B. Tang, Y. Dai, Y. Sun, H. Chen and Z. Wang, *J. Solid State Chem.*, 2020, **284**, 121215.
24 C. Avci, J. Ariñez-Soriano, A. Carné-Sánchez, V. Guillerm, C. Carbonell, I. Imaz and D. Maspoch, *Angew. Chem., Int. Ed.*, 2015, **127**, 14625–14629.
25 G. Kumari, K. Jayaramulu, T. K. Maji and C. Narayana, *J. Phys. Chem. A*, 2013, **117**, 11006–11012.
26 Y. Su, H. Zhu and H. Dong, *Anal. Lett.*, 2015, **48**, 477–488.
27 V. A. Tran, K. B. Vu, T. T. T. Vo, H. H. Do, L. G. Bach and S. W. Lee, *Appl. Surf. Sci.*, 2021, **538**, 148065.
28 D. P. Al Rodrigues, M. G. Rodrigues, P. F. Tomaz and T. L. Barbosa, *Curr. Nanomater.*, 2021, **6**, 66–73.
29 F. Y. Ünlü and A. Aydogan, *ACS Appl. Polym. Mater.*, 2023, **5**, 7193–7200.